01

Features of the penetration of elements of the cumulative jet into a steel barrier

© V.I. Kolpakov,[1] I.R. Kagarmanov,[1,2] I.A. Semenov[2]

[1] Bauman Moscow State Technical University,
105005 Moscow, Russia
[2] NPO Bazalt,
105318 Moscow, Russia
e-mail: isk4344@yandex.ru

Received April 10, 2022
Revised April 10, 2022
Accepted May 19, 2022

Based on numerical simulations carried out using numerical methods of continuum mechanics, the influence on the depth of craters, formed in steel barriers of various strengths, geometric and kinematic parameters of elongated cylindrical copper strikers, simulating elements of a cumulative jet, in the range from 0.3 to 8 km/s. For description the behavior of materials of the impactor and barrier, the model of a compressible elastic-plastic medium with a variable value of the yield strength. Determined that the classical hydrodynamic theory of the penetration of a cumulative jet into a barrier is not takes into account the effects of the inertial movement of the barrier after triggering separately taken element (aftereffect). The existence of three regimes is distinguished shock interaction-high-speed, when the elements behave like a liquid body, are worked out, but not inhibited; low speed, when the elements behave like solid body and are decelerated as a whole and intermediate, when the elements are decelerated and are deformed at the same time. It is shown that the braking mode of copper elements at high-speed impact on a steel armored barrier is realized at speeds smaller 0.8−1 km/s. It is shown that when interacting with an obstacle, high-speed fragmented cumulative jet, the total depth of armor penetration will be greater, than this is predicted by the classical hydrodynamic theory of penetration, and the more more, the higher the speed of the elements and the greater the distance between them on the one hand and less strength of the barrier on the other side.

Keywords: High-velocity strike, elongated striker, cumulative jet, steel barrier, crater, inertial movement of the barrier, numerical modeling.

DOI: 10.21883/TP.2022.09.54674.92-22

Introduction

Cumulative jets (CJs), formed when cumulative charges (CCs) are initiated, in the course of their evolutionary development successively go through the stages of stretching and fragmentation. Fragmentation of the CJ occurs into a finite number of elements, which subsequently do not change their length. In this case, the head high-speed part, as a rule, of copper CS interacts with the obstacle without loss of its continuity, and its tail sections participate in the process of armor penetration in the form of a stream of elements moving one after another [1,2]. The range of velocities of the elements of the fragmented part of the copper CJ is 1−5 km/s.

When the cumulative jet penetrates into a steel obstacle for its high-speed sections with a speed of $v_S > 4-5$ km/s, the influence of the strength of the interacting materials can be neglected [1–4]. In this case, the introduction of the CJ is described by the hydrodynamic theory of penetration, in which the materials of the jet and obstacles are considered ideal incompressible fluids, and in the assumption that the process is stationary, the Bernoulli equation is used, which has the form

$$\frac{1}{2}\rho_S(v_S-u)^2=\frac{1}{2}\rho_B u^2, \tag{1}$$

where ρ_S, ρ_B — densities of the jet and obstacle; v_S — speed of CJ; u — penetration speed (speed of the point of jet contact with the obstacle along the axis of symmetry of CJ). At that, it is assumed that for a jet element having a length l_S and speed v_S, the penetration (initiation) process is completed during time

$$t_S=\frac{l_S}{v_S-u}.$$

In this case, in the obstacle a cavity is formed with a depth of

$$L=ut_S=\frac{ul_S}{v_S-u}. \tag{2}$$

Expression (1) implies the relation

$$\frac{u}{v_S-u}=\sqrt{\frac{\rho_S}{\rho_B}},$$

which, taking into account (2), is transformed to the form called the Lavrentiev formula

$$L=l_S\sqrt{\frac{\rho_S}{\rho_B}}. \tag{3}$$

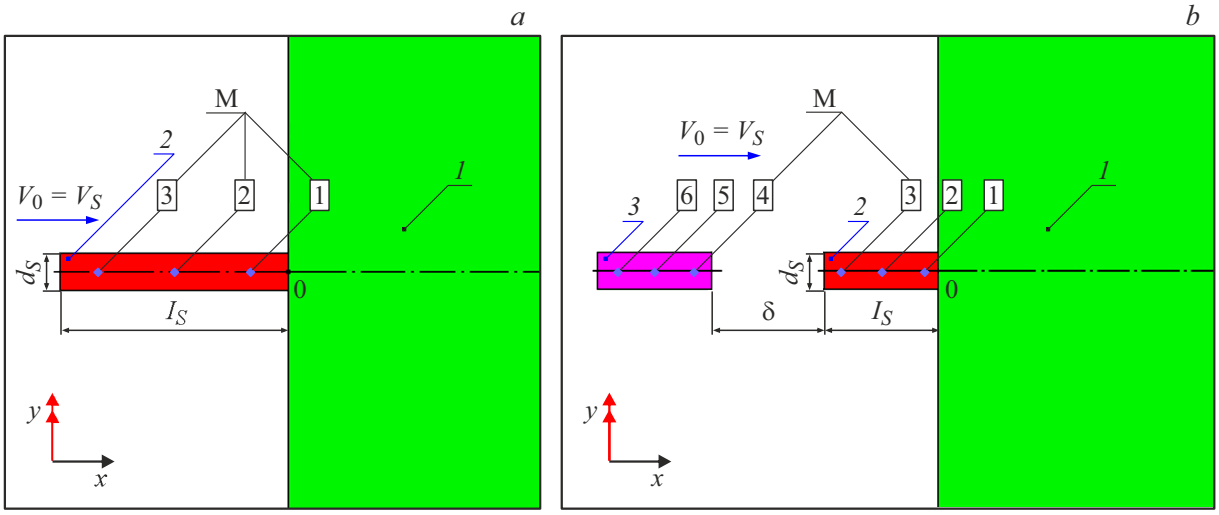

Figure 1. Calculation schemes of impact interaction of one (a) and two strikers (b) with the obstacle, where *1* — obstacle; *2, 3* — strikers; M (№1–6) — movable reference points (markers); $v_0 = v_S$ — initial speed of strikers; d_S, l_S — diameter and length of the striker; δ — distance between strikers; „0“ — starting point of the impact interaction scheme.

The Lavrentiev formula has proven itself well for calculating the depth of CJ penetration into various obstacles. According to (3) the penetration depth is an independent value of the jet speed and the strength characteristics of the obstacle, therefore, the following contradictions are incorporated in the Lavrentiev formula in the case of the obstacle penetration by individual elements of CJ (strikers). On one hand, the kinetic energy of the striker must be converted into work to deepen the cavity (overcome of resistance forces) and to heat the obstacle. Therefore, the penetration depth should increase with striker speed increasing. Known empirical dependencies commit this fact. For example, in the paper [1] to describe the crater scheme for the striker penetration into a steel obstacle a dependence of the following form was suggested

$$L = 5.25(mv^2)^{1/3},$$

where m is striker weight, [g]; v is speed, [km/s]; L is penetration depth, [mm].

On the other hand, it should be noted that in expression (2) the armor penetration depth L is limited by the response time of the jet element t_S. By this time, the obstacle layers adjacent to the contact surface separating the striker and obstacle surfaces are still in inertial motion. Therefore, during the aftereffect period (after the striker initiation moment), the cavity will continue to expand and to deepen until full stop of all layers of the obstacle adjacent to the contact surface. Dependence (3) does not take this effect into account. However, if we imagine the CJ as a continuous flow of individual elements, then after one of them is initiated by the obstacle, its interaction with the next element immediately begins. In this case, the aftereffect period is not realized.

1. Formulation of problem

The aftereffect influence on armor penetration in this paper was evaluated by numerical simulation of the impact interaction process using the ANSYS-AUTODYN software package in a two-dimensional axisymmetric modeling in the Euler coordinate system. In this case, two calculation schemes were used, schematically shown in Fig. 1.

Copper cylinders with a diameter of $d_S = 2$ mm, but of different lengths were used as typical elements of the CJ. In the first scheme the length of the cylinder was $l_S = 12$ mm, and in the second scheme — $l_S = 6$ mm. As the equations of state of the steel obstacle and copper elements, a linear barotropic dependence of the following form was used

$$p = K\left(\frac{\rho}{\rho_0} - 1\right),$$

where K is bulk compression modulus; ρ_0, ρ is initial and current values of material density. For steel the bulk compression modulus was assumed to be $K = 159$ GPa, and the initial density — $\rho_0 = 7.83\,\mathrm{g/cm^3}$; for copper — $K = 129$ GPa and $\rho_0 = 8.93\,\mathrm{g/cm^3}$.

The elastoplastic Johnson–Cook model with a variable yield strength was used to describe the stress-strain state of the materials of CJ elements and the obstacle [5]

$$Y = (A + B\varepsilon_p'')(1 + C\ln\xi_p)(1 - T_{\mathrm{H}}^m), \qquad (4)$$

where Y is dynamic yield strength of the material; $T_{\mathrm{H}} = (T - T_0)/(T_m - T_0)$ is homologous temperature; ε_p is true plastic deformation; ξ_p is deformation rate; T_m is melting point; T_0, T is initial and current temperatures; A, B, C, n, m are empirical constants.

2. Evaluation of the inertial motion of steel obstacle on armor penetration of CJ elements

Fig. 2 shows the results of numerical simulation of the process of impact interaction of a cylindrical element 12 mm long (Fig. 1, *a*) with the obstacle in the range of speeds 0.3−8 km/s, illustrating the change in the final depth of the cavity L_1, taking into account the aftereffect period, depending on the initial speed of the striker v_S. In this case, armored steel of medium hardness and structural steel of medium hardness 40KhNMA, described by the plasticity model (4) with the following numerical values of empirical constants, were used as an obstacle: for armored steel — $A = 0.86$ GPa, $B = 3.5$ GPa; for structural steel — $A = 0.79$ GPa, $B = 0.51$ GPa. The remaining parameters in expression (4) for both steel grades were assumed to be the same and equal to $n = 0.26$, $C = 0.014$, $m = 1.03$, $T_m = 1793°$K. For copper elements similar parameters of the Johnson−Cook model took the following numerical values: $A = 0.09$ GPa, $B = 0.292$ GPa, $n = 0.31$, $C = 0.025$, $m = 1.09$, $T_m = 1356°$K.

The solid line in Fig. 2 marks the calculation data for structural steel 40KhNMA, and the dashed line — for armored steel of medium hardness. It can be seen from the Figure that with the element speed increasing, the depth of the cavity increases. However, at low initial striker speeds ($v_S < 1$ km/s) the penetration process practically stops, which corresponds to the experimentally established level of the critical penetration speed for CJ. Besides, it follows from the analysis of Fig. 2 that for the softer steel 40KhNMA, at the same penetration speed of the striker the cavity has a greater depth than for the harder armored steel (the solid line is above the dashed line). This fact also agrees with the experimental results.

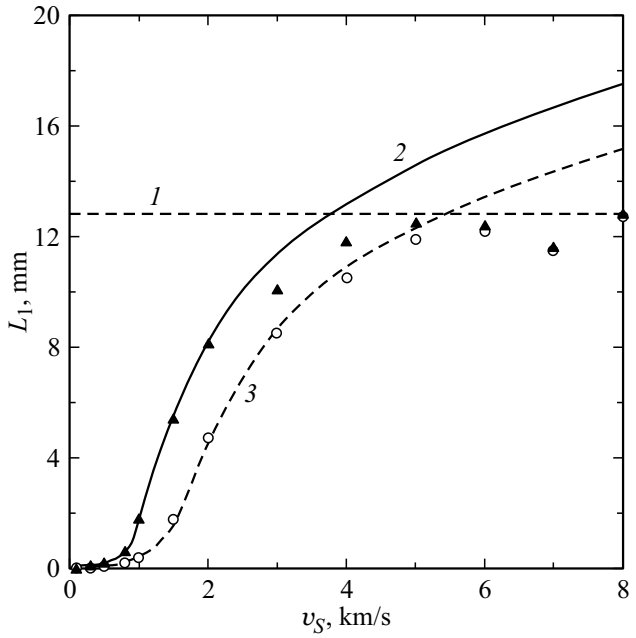

Figure 2. Dependencies characterizing the speed effect on the penetration depth of CJ element: *1* — $L_B = 12.8$ mm; *2, 3* — L_1 for steel 40KhNMA and armor steel, respectively; ▲ — L_C for 40XHMA; ○ — L_C for armor steel.

For CJ element 12 mm long the armor penetration depth calculated by formula (3) is $L_B = l_S\sqrt{\rho_S/\rho_B} = 12\sqrt{8.93/7.83} = 12.8$ mm. In Fig. 2 it is shown by a horizontal dashed line. According to the hydrodynamic theory of penetration, the specified depth corresponds to the moment of full initiation of the striker. Besides, in the above Figure, filled triangles and transparent circles show the calculated values of the depths of cavities in the obstacle, determined at the moment of full initiation of elements moving at different speeds, not considering the inertial expansion of the cavity (parameter L_C). In this case, the triangles correspond to structural steel 40KhNMA, and the circles correspond to armor steel.

From the analysis of the data presented in Fig. 2 it follows that at low striker speeds, the cavity depth at the moment of the striker full initiation (parameter L_C) practically coincides with the lines characterizing the level of the end depth of the cavity L_1, taking into account the aftereffect period. For steel 40KhNMA this range of speeds corresponds to the values $v_S < 2$ km/s; and for armored steel — $v_S < 4$ km/s. For higher penetration speeds ($v_S > 4$ km/s) the aftereffect period plays a more significant role in the process of armor penetration. At the same time, for the considered steel obstacles the difference in the values of L_C and L_1 increases, and the value of the parameter L_C reaches a constant level, approximately equal to the armor penetration depth calculated by the Lavrentiev formula. It should also be noted that the nonmonotonicity in the behavior of the numerical values L_C in Fig. 2 is due to the error in establishing the moment of complete initiation of the CJ element during calculations.

Thus, the results of direct mathematical modeling of the penetration process of the elongated CJ element into steel obstacles confirm the assumption that the Lavrentiev formula is valid for high-speed sections of the CJs if they represent a continuous flow of discrete elements. In this case, after each individual element is initiated against the obstacle, interaction with the next element immediately begins. In this case, the aftereffect period is not realized. On the whole, the results of the performed mathematical modeling confirm the validity of the main provisions of the hydrodynamic theory, which describes the process of penetration of high-velocity parts of CJ ($v_S > 4$ km/s) into the obstacle.

3. Assessment of strength effects on penetrating capacity of CJ elements

At low jet speeds ($v_S < 4$ km/s), which are typical for its middle and tail sections, strength effects begin to play a significant role. Besides, in this case, as noted above, not a

continuous jet, but a stream of elements is introduced into the steel obstacle. In the first approximation, the strength properties of the materials of the obstacle and the CJ can be taken into account by modifying the hydrodynamic model of penetration. At the same time, following the paper [3], the Bernoulli equation, modified in accordance with the Alekseevsky–Tate approach, can be written in the form

$$\frac{1}{2}\rho_S(v_S-u)^2+Y_S=\frac{1}{2}\rho_B u^2+H_D, \qquad (5)$$

where H_D is dynamic hardness of the armored steel obstacle material; Y_S is dynamic yield strength of jet material. The parameter H_D in the expression (5) is interpreted as the strength resistance of the obstacle to the penetration of CJ elements. Note that the condition $H_D \gg Y_S$ is satisfied when CJ copper element is introduced into the armored steel obstacle.

The depth decreasing of CJ penetration with the obstacle strength increasing is determined by the ratio of the dynamic hardness of the obstacle to the pressure of complete deceleration of the cumulative jet. This dimensionless ratio is called the Euler number (criterion):

$$\mathrm{Eu}=\frac{2H_D}{\rho_S v_S^2}. \qquad (6)$$

The strength resistance of the obstacle stops the penetration of CJ elements when the brake pressure generated by them becomes equal to the dynamic hardness of the obstacle, i.e., at $\mathrm{Eu}=1$. The maximum residual speed of the CJ, when armor penetration stops, is called critical. The critical penetration speed can be estimated using the formula

$$v_{CR}=\sqrt{\frac{2H_D}{\rho_S}}. \qquad (7)$$

To carry out calculations using formula (7), it is necessary to determine the value of the dynamic hardness of the obstacle H_D. According to R. Hill's formula, for steel the value H_D is related to the dynamic yield strength Y_B by the dependence $H_D=3Y_B$ [3]. The numerical value Y_B, in its turn, relates to the static yield strength $\sigma_{0.2}$ by the relation [4]

$$Y_B=(1.5-2)\sigma_{0.2}.$$

The result is an estimate

$$H_D=(4.5-6)\sigma_{0.2}.$$

According to the last expression, at $\sigma_{0.2}=0.86\,\mathrm{GPa}$ [3] the estimate of the dynamic hardness value for armored steel of medium hardness is $H_D=3.9-5.2\,\mathrm{GPa}$, and the value of critical speed for copper CJ, calculated by formula (7) at copper density $\rho_S=8.93\,\mathrm{g/cm^3}$, equals $v_{CR}=0.93-1.08\,\mathrm{km/s}$. Note that the existing experimental estimates of the critical speed for the penetration of the armored steel by elements of the copper CJ according to different sources have a significant spread and vary from 1 to 3 km/s.

Let us describe the nature of the state change of the CJ elements themselves during penetration. To do this, we will use the modification of the Euler number (6):

$$\mathrm{Eu}_S=\frac{2Y_S}{\rho_S v_S^2}.$$

When the inertial forces of the CJ element (striker) greatly exceed the force of its internal resistance, i.e., when the condition is met

$$\frac{1}{2}\rho_S v_S^2 \gg Y_S \text{ or } \mathrm{Eu}_S \ll 1 \text{ (i.e. } \mathrm{Eu}_S \approx 0),$$

the material of the element during impact behaves like a liquid body. In this case, only the front part of the striker, which is in contact with the obstacle, experiences braking. The tail part of the striker at the same time continues movement at the current speed.

At a low-speed impact, i.e., under the condition

$$\frac{1}{2}\rho_S v_S^2 \ll Y_S \quad \text{or} \quad \mathrm{Eu}_S \gg 1,$$

the material of the jet element behaves like a solid body. In this case, the entire element is decelerated, i.e., during the impact the speeds in all its parts are the same and gradually decrease with time.

At intermediate speeds of the striker determined by the conditions

$$\frac{1}{2}\rho_S v_S^2 \approx Y_S \quad \text{or} \quad \mathrm{Eu}_S \approx 1,$$

there is a transition region when the CJ element starts to decelerate upon impact and simultaneously to wear out or to deform. This region corresponds to the condition

$$\frac{1}{2}\rho_S v_S^2 \approx Y_S$$

and characteristic penetration speed

$$v_{S0}=\sqrt{\frac{2Y_S}{\rho_S}}. \qquad (8)$$

For the copper CJ element, according to formula (4), at $\sigma_{0.2}=0.09\,\mathrm{GPa}$, the dynamic yield strength is equal to $Y_S=(1.5-2)\sigma_{0.2}=135-180\,\mathrm{MPa}$. In this case, the characteristic speed is equal to $v_{S0}=174-200\,\mathrm{m/s}$. According to the data of paper [5], the dynamic yield strength for copper when the SJ penetrates into the steel obstacle is about 0.4 GPa, and in the paper [6] a value of 0.2 GPa is used. In these cases, the numerical values v_{S0} are $v_{S0}=212-300\,\mathrm{m/s}$.

Comparison of formulas (7) and (8) shows that the critical penetration speed for the copper jet element (v_{CR}) is much higher than its characteristic speed (v_{S0}). Therefore, according to the estimates made the jet elements that have speed above the critical one and are still capable of armor penetration, will behave like liquid bodies during initiation, i.e., continue to move at the current speed.

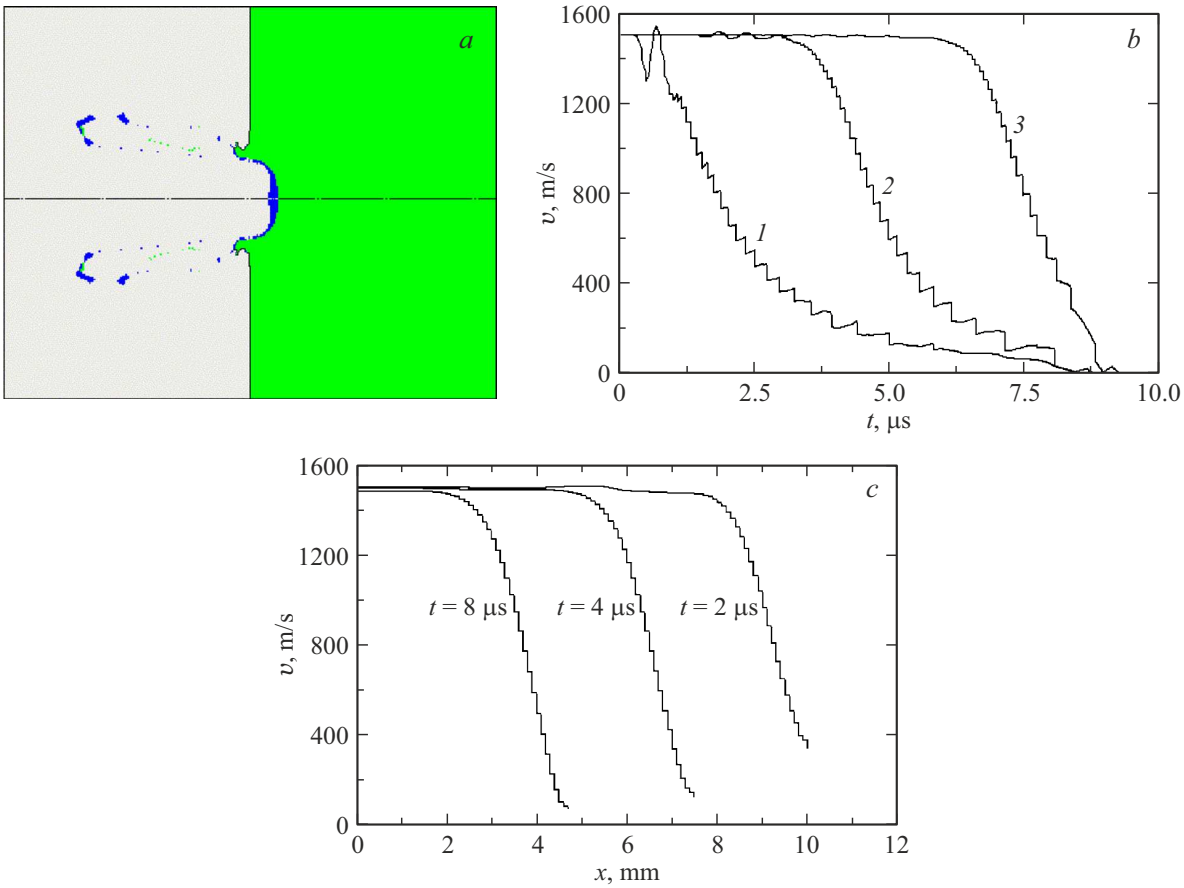

Figure 3. The introduction of the CJ element into the armor obstacle at speed of $v_0 = 1500$ m/s: *a* — final position of interacting materials ($t = 25\,\mu$s); *b* — dependences of speed change on time for moving markers (*1–3*); *c* — distributions of speeds along the length of the element at different times.

The assessment of the degree of influence of strength effects on the penetrating ability of CJ elements moving at different speeds was also carried out in a two-dimensional axisymmetric modeling using the ANSYS-AUTODYN software package. For this, the calculation diagram shown in Fig. 1, *a* was used. In this case, as during the aftereffect evaluation, the copper cylinder with a diameter of 2 mm and 12 mm long (pos. 2) was used as a typical element, and armored steel was used as the obstacle. The initial speed of the element (v_0) is directed along its longitudinal axis of symmetry (left−right) and varied in the range of 1.5 to 0.5 km/s. Besides, the Figure shows movable reference points (markers) and steel obstacle (pos. 1). With the help of movable markers installed along the longitudinal axis of the element at a distance of 2, 6 and 10 mm from its right end, the change in the speed of various parts of the CJ element during its interaction with the obstacle was recorded.

Figs. 3−5 below show the results of numerical simulation of the impact interaction process. Note that the speed of sound in copper is $c_0 = 3.94$ km/s. Therefore, for the described range of initial penetration speeds ($v_0 \leq 1.5$ km/s) the motion of the CJ element has a subsonic character, and upon impact on the material of the striker (CJ element), a sound compression wave begins to propagate from the front end to the rear one, transmitting s to it information about the impact after a time interval of $\Delta t = l/c_0 \approx 3\,\mu$s.

Fig. 3 illustrates the process of the CJ element penetration into the obstacle with the initial speed of $v_0 = 1.5$ km/s. At the same time, Fig. 3, *a* shows the final state of the element and the obstacle, and Fig. 3, *b* shows the time dependences of the change in speed at the reference points of the element. Fig. 3, *c* for different moments of time shows the distribution of speeds along the length of the CJ element (x) that did not initiate yet, which is counted from its rear end. In this case, the length of the element itself is constantly decreasing with time.

It can be seen from Fig. 3, *a* that a cavity formed in the obstacle, and the CJ element completely wear out and spread over its walls. The analysis of the graphical dependences presented in Fig. 3, *b, c* shows that the rear sections of the CJ element, when it penetrates into the obstacle, are practically not decelerated, and in the head part of the element located in the immediate vicinity from the contact surface with the obstacle there is a transition section, the width of which is about 2.5−3 mm. Along this section, the speed of the striker sharply decreases, and its material experiences severe plastic deformations. At the

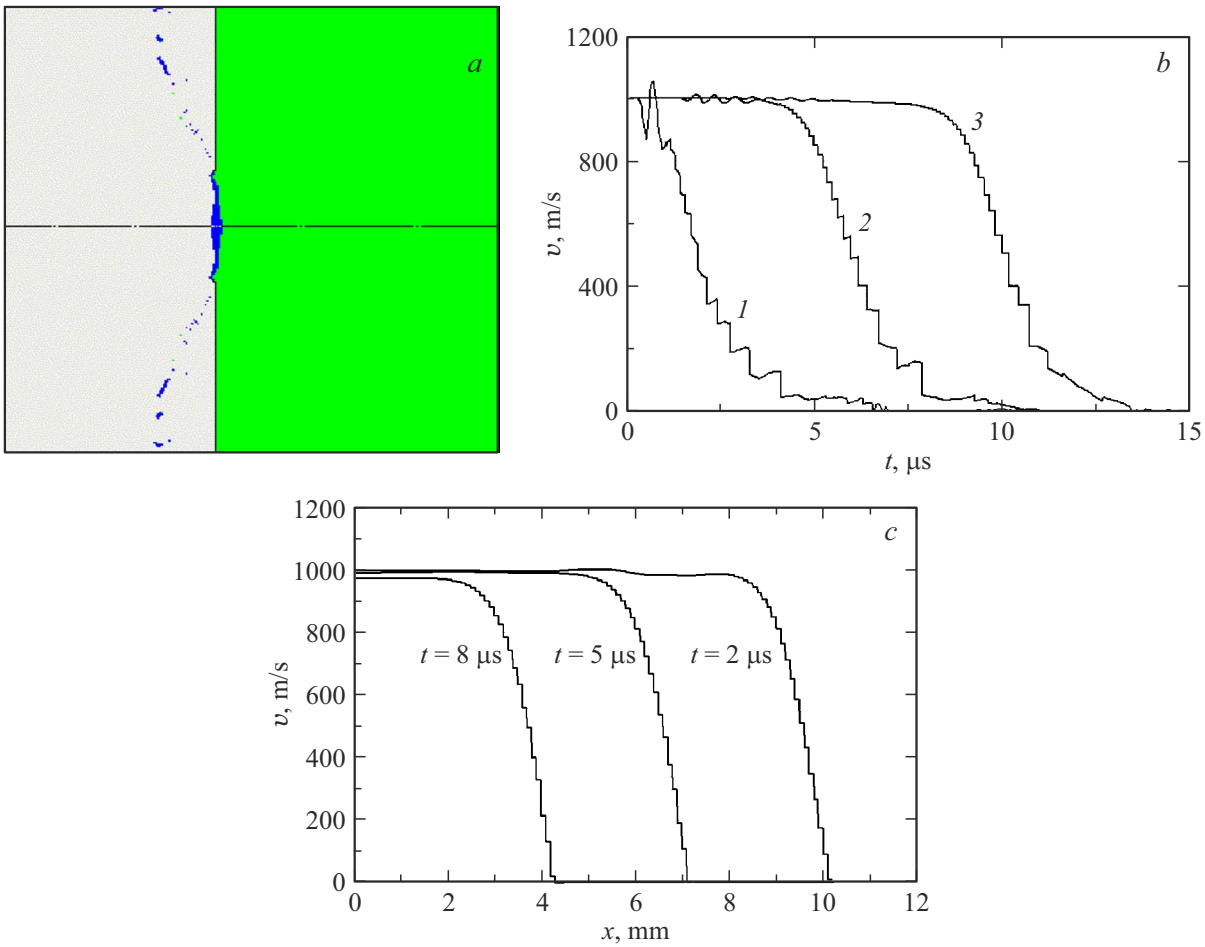

Figure 4. The introduction of the CJ element into the armor obstacle at a speed of $v_0 = 1000$ m/s: *a* — final position of interacting materials ($t = 25\,\mu$s); *b* — dependences of speed change on time for moving markers (*1*–*3*); *c* — distributions of speeds along the length of the element at different times.

same time, the material of the rear region is in an elastic state.

Fig. 4 shows the results of calculations of the impact interaction with the initial speed of $v_0 = 1.0$ km/s, illustrating that in this case there is practically no cavity in the obstacle (Fig. 4, *a*). Consequently, the initial speed of the CJ element penetration into the obstacle in this case is close to the numerical values of the critical speed of armor penetration. In this case, the rear sections of the element decelerate slightly when they penetrate into the obstacle (Fig. 4, *b, c*).

Fig. 5 shows the results of calculations of the process of the CJ element penetration into the obstacle with the initial speed of $v_0 = 0.5$ km/s. It can be seen from Fig. 5, *a* that in this case the obstacle is not penetrated, and the striker after stop takes the form of a „cake". Besides, the analysis of data shown in Fig. 5, *b, c* indicates that at given impact speed, the rear sections of the CJ element are significantly decelerated during the impact.

Note that the results of the performed calculations are in accordance with the previously presented theoretical estimate of the numerical value of the critical speed ($v_{CR} = 0.93-1.08$ km/s). Indeed, as can be seen from Fig. 3 that at the initial striker speed $v_0 = 1.5$ km/s the cavity in the obstacle is still formed, and at $v_0 = 1.0$km/s it is practically absent (Fig. 4).

Thus, based on the results of the performed calculations, it can be concluded that in the high-speed mode of penetration, when the inertial forces of the cumulative jet element (striker) considerably exceed the forces of its internal resistance, the material of the element behaves like a liquid body. In this case, only the front part of the striker, which is in contact with the obstacle, experiences braking. At the same time the tail part of the striker continues to move at the initial speed, i.e., the material of the striker wears out, but is not decelerated.

4. Results of calculations of interaction with the obstacle fragmented by CJ

As noted above, when interacting with CJ fragmented obstacle, which is stream of elements separated from each other by an air gap, the aftereffect period begins to play

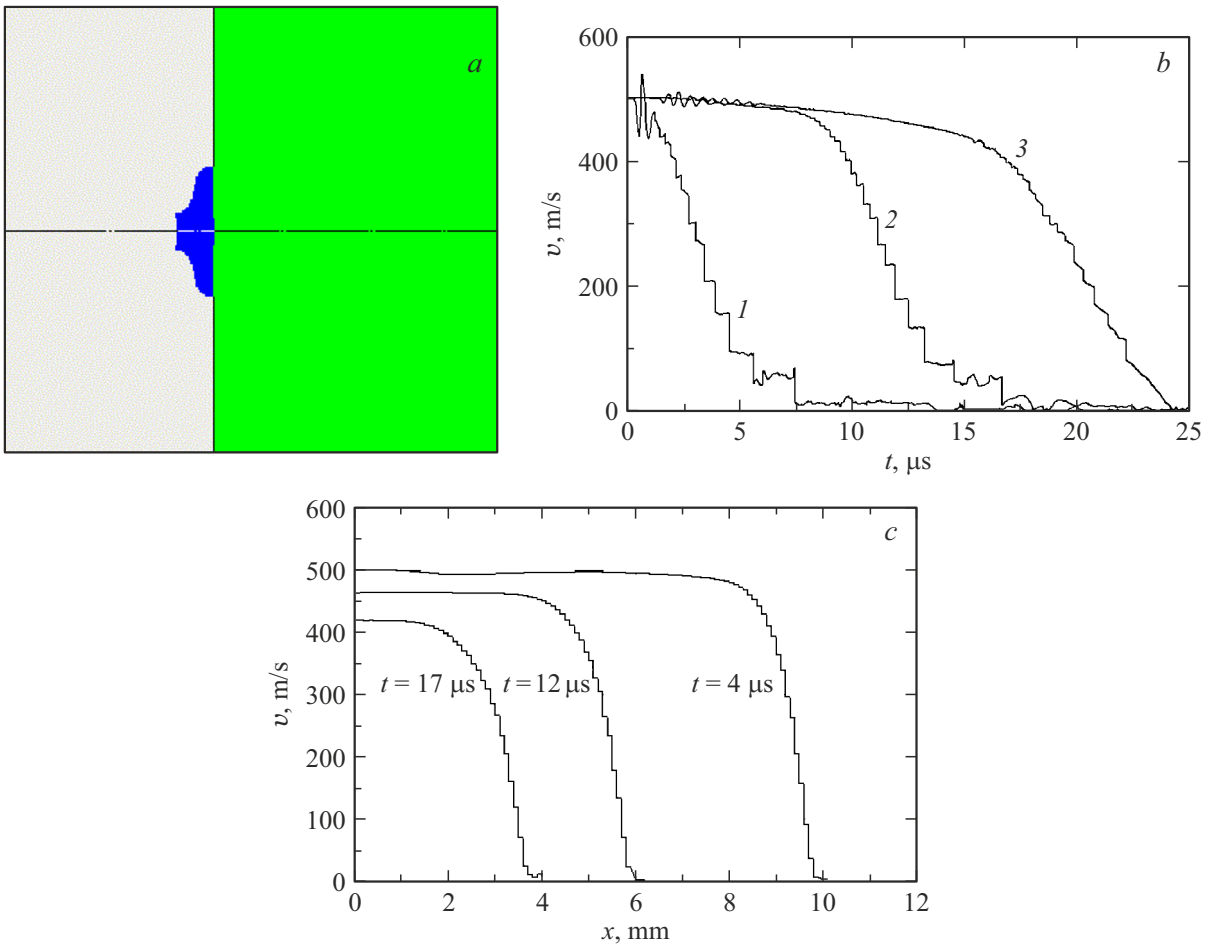

Figure 5. The introduction of the CJ element into the armor obstacle at a speed of $v_0 = 500$ m/s: *a* — final position of interacting materials ($t = 25\,\mu$s); *b* — dependences of speed change on time for moving markers (*1*–*3*); *c* — distributions of speeds along the length of the element at different times.

a more significant role in the process of armor penetration than when its individual elements penetrate. Therefore, in this case, it can be expected that the total depth of armor penetration will be greater than when calculated using the Lavrentiev formula.

To confirm this statement the computer simulation of the process of penetration into various steel obstacles of two identical cylindrical elements with diameter of $d_S = 2$ mm and $l_S = 6$ mm long, located coaxially one after another at different distances and moving with the same speed (Fig. 1, *b*), was made. In the calculations the speed and distance between the elements (δ) varied in the range of 0 to 18 mm ($0 \le \delta/l_S \le 3$). In this case, the total depth of penetration of elements L was determined. The results of calculations in the form of illustrations are presented in Fig. 6, *a* in the form of graphs $L/L_0 = f(\delta/l_S)$ in Fig. 7, 8 and $L/L_0 = f(v_S)$ in Fig. 9, where L_0 — penetration depth of elements at $\delta = 0$.

As can be seen from Fig. 7, when two consecutive elements penetrate into various steel obstacles, the effect of superposition from their joint action is observed. At the same time, the penetration depth increasing compared to the action of a solid jet ($\delta = 0$) is the greater, the higher the speed of the elements and the greater the distance between them on the one hand and the lower the strength of the obstacle, on the other hand are. The solid lines in this Figure show the calculated graphical dependences of the impact interaction of elements with speeds of 8, 6, 5 and 4 km/s along the armored obstacle, and the dashed lines — along the obstacle made of structural steel 40KhNMA. The superposition effect is observed up to speeds $v_S \approx 2$ km/s (Fig. 8). However, its effect on the total armor penetration depth gradually decreases from 17–19% at a speed of 8 km/s to 1–2% at a speed of 2 km/s. Moreover, as can be seen from Fig. 9, the total effect of the joint action of the CJ copper elements on the obstacle of armored steel at speed less than 4.6–5.2 km/s becomes less than predicted by the hydrodynamic theory of penetration (Fig. 9, *a*). When acting on the obstacle made of structural steel 40KhNMA, the indicated speed range is 3.2–3.8 km/s (Fig. 9, *b*).

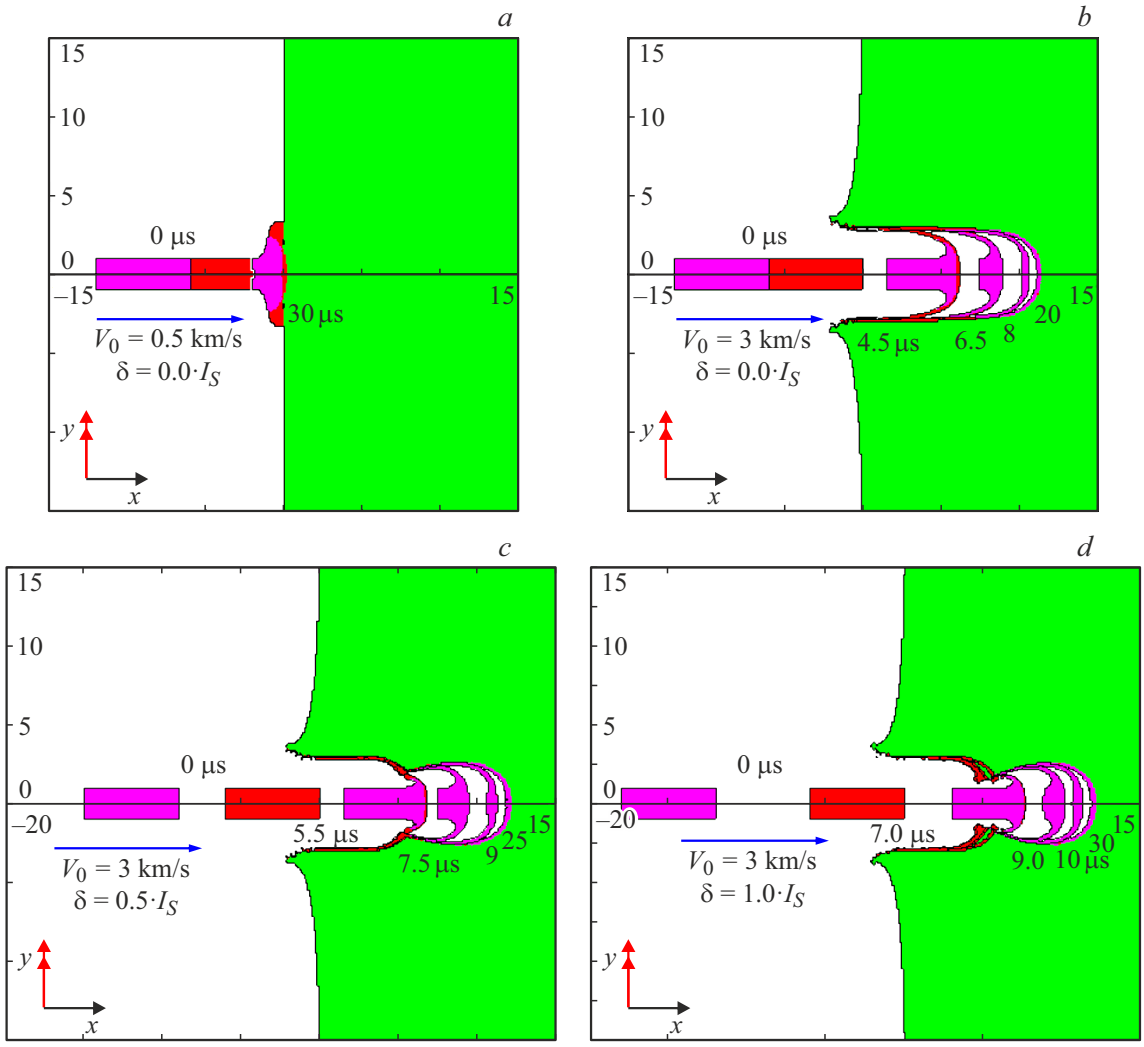

Figure 6. Impact interaction of two copper elements with obstacle made of structural steel 40KhNMA: *a* — $v_0 = v_S = 0.5$ km/s, $\delta/l_S = 0$; *b* — $v_0 = 3.0$ km/s, $\delta/l_S = 0$; *c* — $v_0 = 3.0$ km/s, $\delta/l_S = 0.5$; *d* — $v_0 = 3.0$ km/s, $\delta/l_S = 1.0$.

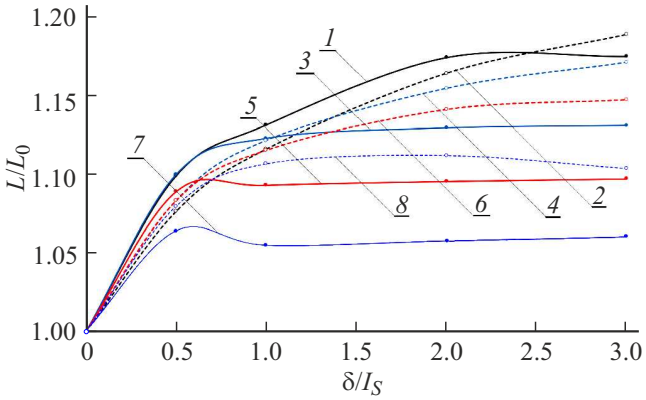

Figure 7. Comparison of the relative penetration depth of various steel obstacles L/L_0 by CJ copper elements from the relative distance δ/l_S between them: *1, 3, 5, 7* — armor steel; *2, 4, 6, 8* — 40KhNMA steel; v_S, km/s: *1, 2* — 8; *3, 4* — 6; *5, 6* — 5; *7, 8* — 4.

The obtained simulation results also show that at interaction speeds below critical no armor penetration occurs, and at speeds above critical the not initiated part of the first element does not experience braking during penetration. A similar effect covers all fragmented CJ elements that can contribute to armor penetration. As a result, at the same speed of the elements, the second element does not come up with the first element and begins its penetration after a certain period of time after the first element is fully initiated.

Note that in contrast to the results presented in earlier papers [2,7,8] a directly opposite statement was made about the mechanism of penetration of fragmented CJ part, which is still capable of armor penetration. At the same time, it was stated that the CJ elements moving as stream are „decelerated“ during their wearing out on the obstacle due to the fact that each subsequent element, somewhat „drops upon“ the previous „decelerated“ element and starts to wear out not on the obstacle, but on the previous element.

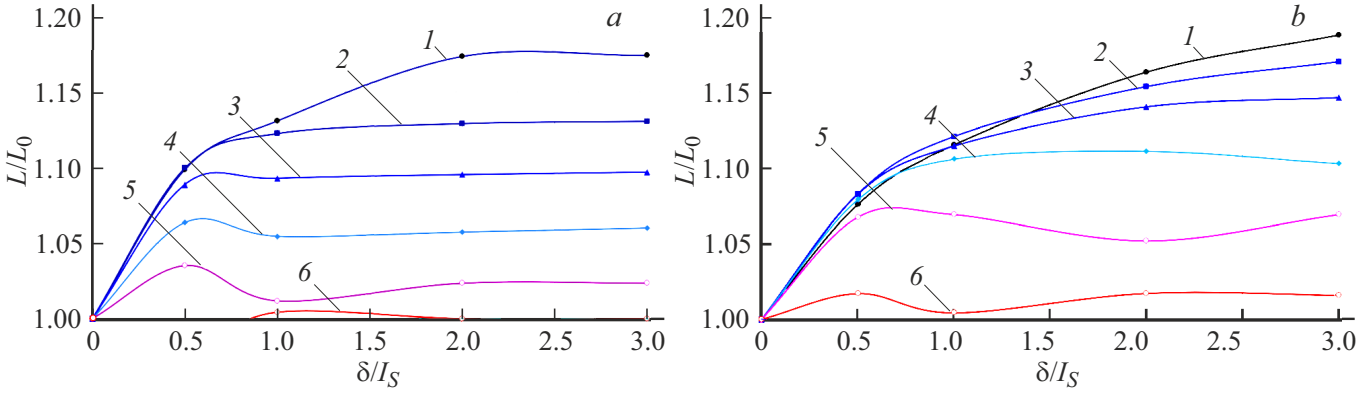

Figure 8. Relative penetration depth of armor obstacle (*a*) and obstacle made of structural steel 40KhNMA (*b*) L/L_0 by CJ copper elements vs. relative distance δ/l_S between them: v_S, km/s: *1* — 8, *2* — 6, *3* — 5, *4* — 4, *5* — 3, *6* — 2.

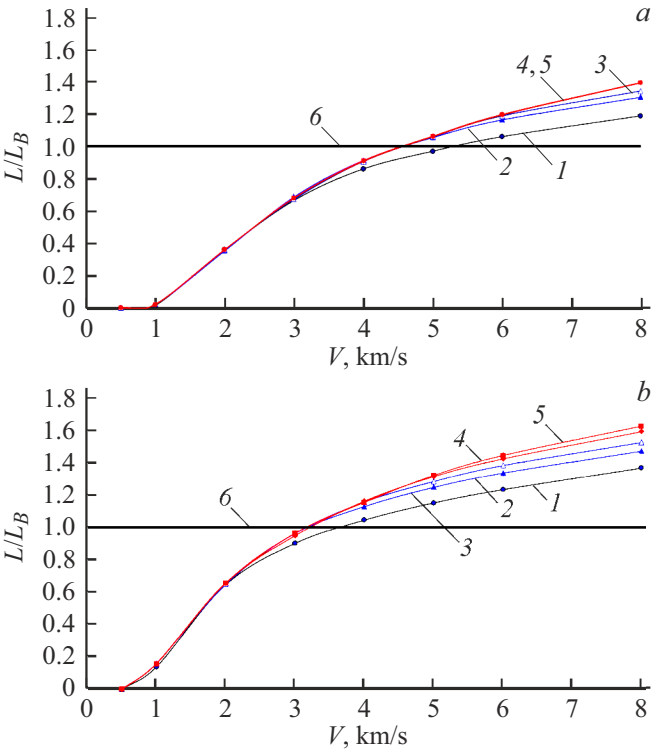

Figure 9. Relative penetration depth of armor obstacle (*a*) and obstacle made of structural steel 40KhNMA (*b*) L/L_B by CJ copper elements vs. speed, δ/l_S: *1* — 0, *2* — 0.5, *3* — 1, *4* — 2, *5* — 3, *6* — theoretical value ($L_B = 12.8$ mm).

As a result, namely the effect of „mutual effect“ leads to the total depth decreasing of armor penetration of the tail section of the CJ. In contrast, the data presented in this paper show that penetration depth decreasing of the rear part of CJ is not due to the effect of the mutual effect of its elements on each other during penetration, but is associated with the strength characteristics of the particular obstacle.

Conclusion

1. The results of mathematical modeling of the process of elongated CJ elements penetration into steel obstacles made of armor steel of medium hardness and structural steel of medium hardness 40KhNMA in a wide range of initial speeds of 0.3–8.0 km/s are presented. It is shown that the classical hydrodynamic theory of the cumulative jet penetration into the obstacle (Lavrentiev formula) does not take into account the effect of the inertial movement of the obstacle after the initiation of the single element of the cumulative jet (the effect of the aftereffect period).

2. The validity of the hydrodynamic theory of penetration is proved only for high-speed sections of the CJ, which is a solid flow of elements following in close proximity to each other. In this case, after each individual element initiation on the obstacle, the next element immediately penetrates, and the effect of the inertial movement of the obstacle during the aftereffect is absent.

3. The existence of three modes of impact interaction of elements of copper CJ with steel obstacle is shown, namely, a high-speed mode, when the elements behave like a liquid body (the material of the striker wears out, but is not decelerated); low-speed mode, when the elements behave like a solid body and are braked as a whole; and an intermediate mode between the first and second ones. In the latter case, the jet elements are decelerated and simultaneously deformed upon impact. It is shown that the mode of deceleration of the CJ copper elements during high-speed impact on steel armor obstacle is realized at speeds less than 0.8–1 km/s.

4. It is shown that „effective“ elements of CJ having a speed above the critical one (0.8–1 km/s) and capable of contributing to armor penetration are not decelerated during the impact. Therefore, the effect of „stream“ deceleration of the CS elements, which is characteristic for its low-speed part, in which each subsequent element, somewhat „drops upon“ the element that precedes it element „decelerated“ against the obstacle, does not affect the depth of armor

penetration of the cumulative charge for the obstacles of medium and high hardness.

5. It is shown that when high-speed fragmented CJ, which is a stream of individual elements separated from each other by an air gap, interacts with the obstacle, the inertial movement of the obstacle during the aftereffect plays a more significant role in the process of armor penetration. In this case, it can be expected that the total depth of armor penetration will be greater than that predicted by the classical hydrodynamic theory of penetration, and the greater, the higher the speed of the elements and the greater the distance between them on the one hand, and the lower the strength of the obstacle, on the other hand, are.

Conflict of interest

The authors declare that they have no conflict of interest.

References

[1] *Fizika vzryva*, pod red. L.P. Orlenko (Fizmatlit, M., 2004), izd. 3, ispr. v 2 t., t. 2, 656 s. (in Russian)
[2] S.A. Kinelovskiy, Yu.A. Trishin. FGV, **16** (5), 26–40 (1980) (in Russian)
[3] *Chastnye voprosy konechnoy ballistiki*, V.A. Grigoryan, A.N. Beloborodko, N.S. Dorokhov [etc.]; under the editorship of V.A. Grigoryan (Izd-vo MGTU im. N.E. Baumana, M., 2006), 592 s. (in Russian)
[4] G.I. Kannel, S.V. Razorenov, A.V. Utkin, V.E. Fortov. *Udarno-volnoviye yavleniya v kondensirovannykh sredakh* (Janus–K, M., 1996), 408 s. (in Russian)
[5] *Metody issledovaniya svoystv materialov pri intensivnylh dinamicheskikh nagruzkakh: Monografiya* pod obsch. red. M.V. Zhernokletov (RFYaTs-VNIIEF, Sarov, 2005), 2 izd., dop. i ispr., 428 s. (in Russian)
[6] L.P. Orlenko, A.V. Babkin, V.I. Kolpakov. *Zadachi prikladnoy gazodinamiki: Rezul'taty chislennogo rescheniya* (MVTU im. N.E. Baumana, M., 1988), 104 s. (in Russian)
[7] I.I. Tomashevich. FGV, **23**,(2), 97–101 (1987) (in Russian)
[8] W.P. Walters, W.J. Flis, P.C. Chou. Int. J. Impact Engineer., **7** (3), 307–325 (1988).